# Supporting Information

## Multiplexed Profiling of Single-cell Extracellular Vesicle Secretion

Yahui Ji[1,2], Dongyuan Qi[3], Linmei Li[1], Haoran Su[1,2], Xiaojie Li[2], Yong Luo[4], Bo Sun[5], Fuyin Zhang[5], Bingcheng Lin[1], Tingjiao Liu*[2], Yao Lu*[1]

[1]Department of Biotechnology, Dalian Institute of Chemical Physics, Chinese Academy of Sciences, Dalian, 116023, China

[2]College of Stomatology, Dalian Medical University, Dalian, 116044, China

[3]First Affiliated Hospital of Dalian Medical University, Dalian, 116011, China

[4]State Key Laboratory of Fine Chemicals, Department of Chemical Engineering & School of Pharmaceutical Science and Technology, Dalian University of Technology, Dalian, 116024, China

[5]Second Affiliated Hospital of Dalian Medical University, Dalian, 116027, China

*Correspondence should be addressed to Y. Lu (luyao@dicp.ac.cn) or T.J.L. (tingjiao@dmu.edu.cn)

www.pnas.org/cgi/doi/10.1073/pnas.1814348116

# Supplementary Figures

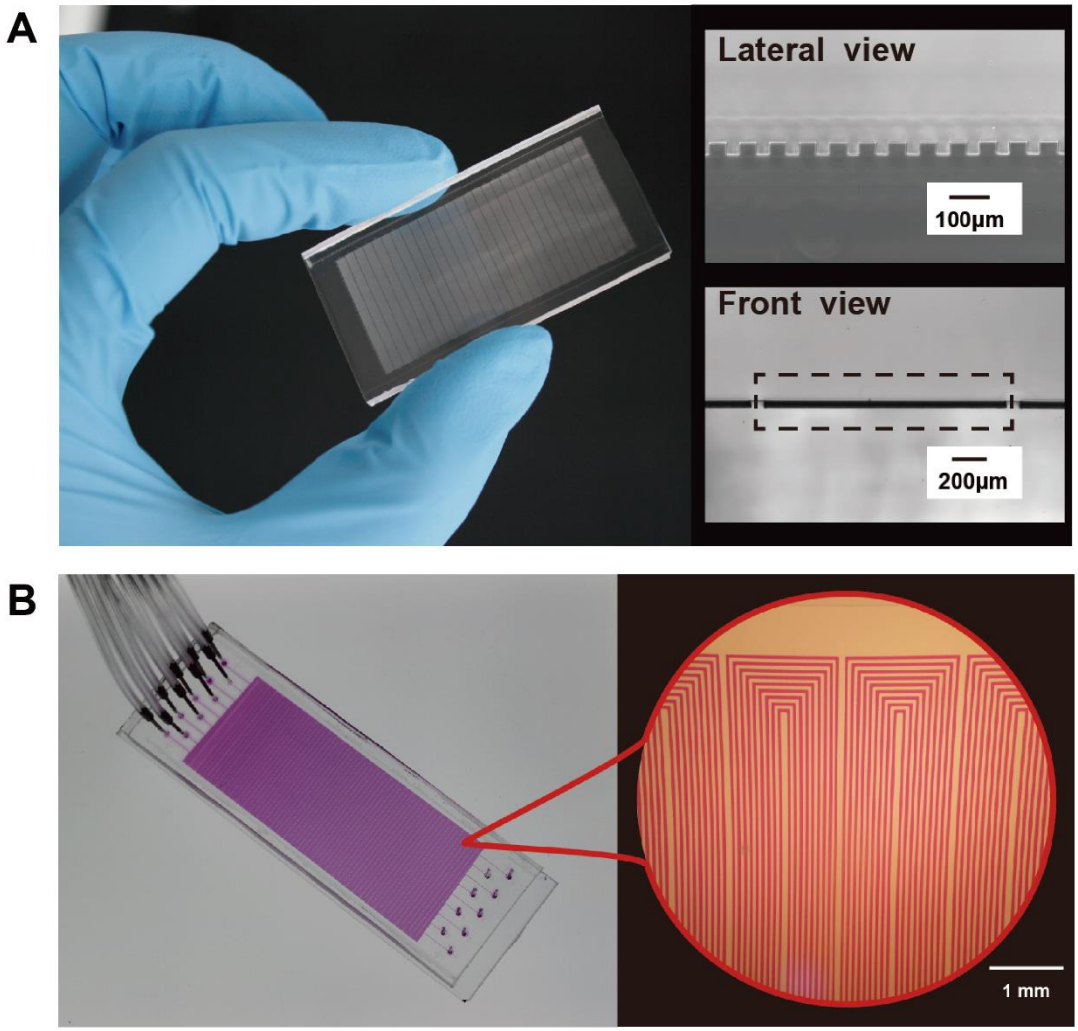


**Figure S1.** Two functional components of microchip platform for multiplexed profiling of single-cell EV secretion. A, Photographs showing the 6343 PDMS microchambers array to isolate and concentrate EVs secreted from thousands of single cells; B, Images showing the highly parallel microchannel array to pattern spatially resolved antibody barcodes glass slide (the microchannels were filled with red dye solution for visualization).

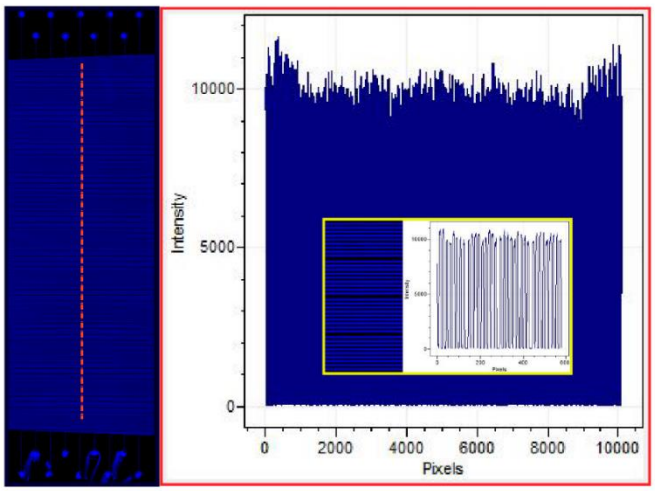


**Figure S2.** The uniformity characterization of protein patterning on a poly-L-lysine glass slide by flow patterning (C.V. <5% across 2 cm x 5.5 cm area). 3μL fluorescently labeled bovine serum albumin (FITC-BSA, 0.25 mg/mL) was pushed through nine parallel microchannels under one psi $N_2$ until completely dry. After blocking and washing, it was scanned and analyzed by GenePix 4300A and GenePix Pro software (Molecular Devices).

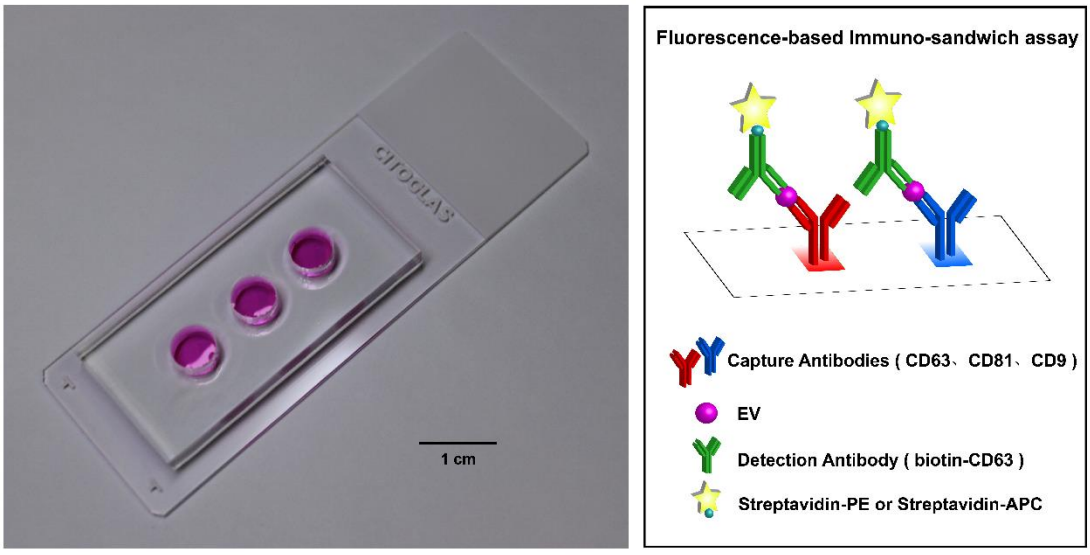


**Figure S3.** Device and detection principle of cell population EV secretion assay. Assembly of PDMS microwells slab (diameter=7mm) with poly-L-lysine glass slide for EV detection with samples from population cells (Left). Schematic illustrating double positive detection strategy based on different epitopes recognition for EV detection (right).

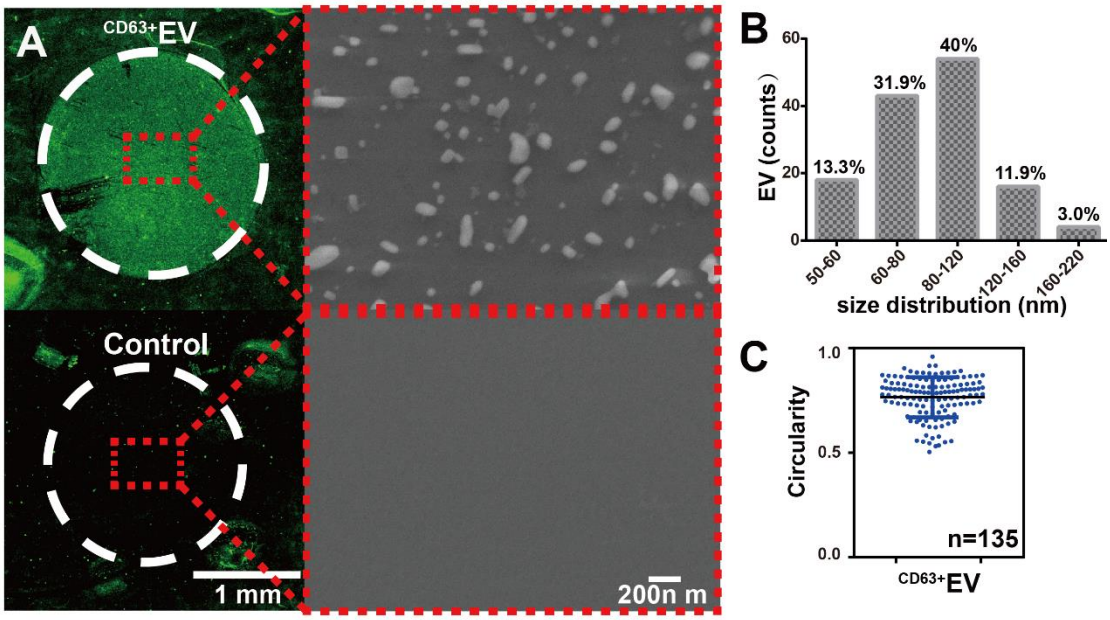


**Figure S4.** Characterization of captured EVs on anti-CD63 antibody-coated spots (circled fluorescence detection regions) with SEM. A, EV detection results on anti-human CD63 antibody-coated spot with SCC25 cells conditioned medium and control sample (blank cell culture medium supplemented with 10% ultra-centrifuged FBS): fluorescence and SEM. B, C, The size and circularity distribution of extracellular vesicles captured on the spot.

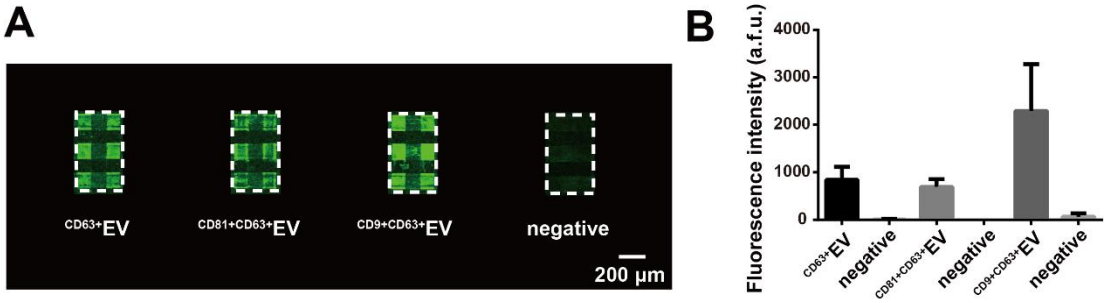


**Figure S5.** Validation of CD63, CD9, CD81 antibody barcodes to capture/detect EVs from UM-SCC6 supernatant. A: Fluorescence images and B: quantification.

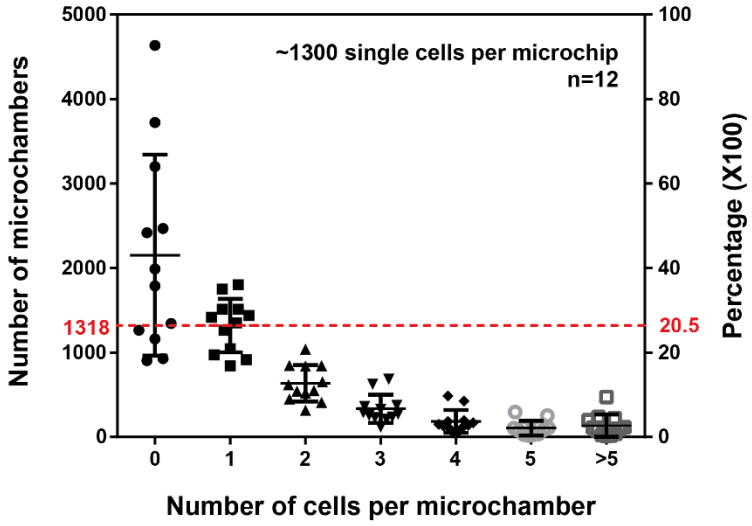


**Figure S6.** Distribution of the number of cells across a whole microchip, from which we can see more than 1000 single cells (20.5%, 1318±317, n=12, red dashed line) were constantly obtained in one microchip.

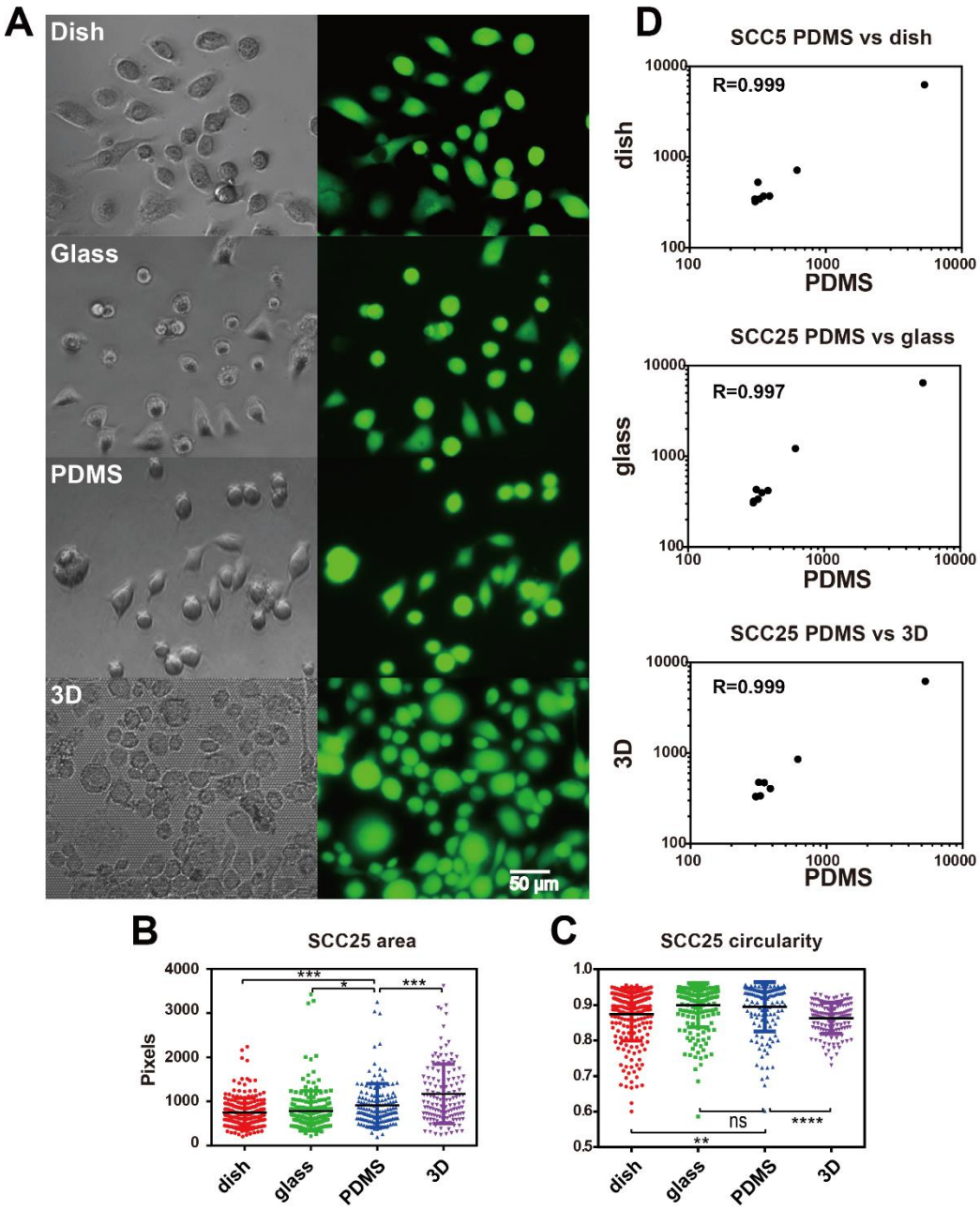


**Figure S7.** Comparison of SCC25 cells cultured at different substrates. A-C, Morphology analysis of the cells, including A: optical & viability fluorescence staining; B: spread area, and C: cell circularity (n=220, 186, 145, 136 for the Petri dish, glass, sealed PDMS chamber, and 3D culture plate (SCIVAX's NanoCulture Plate)). D, Bulk level secretion analysis (including $^{CD63+}$EV, $^{CD9+CD63+}$EV, $^{CD81+CD63+}$EV, $^{EpCAM+CD63+}$EV, $^{HSP70+CD63+}$EV, IL-8, IL-6, and MCP-1), which showed there're no significant differences in secretion between the SCC25 cells cultured in sealed PDMS chambers and the cells cultured on Petri dish, glass or 3D cell culture plate (P=0.741,0.4816, and 0.5051, paired t-test) and they exhibited high correlation with each other (R=0.999, 0.997, and 0.999).

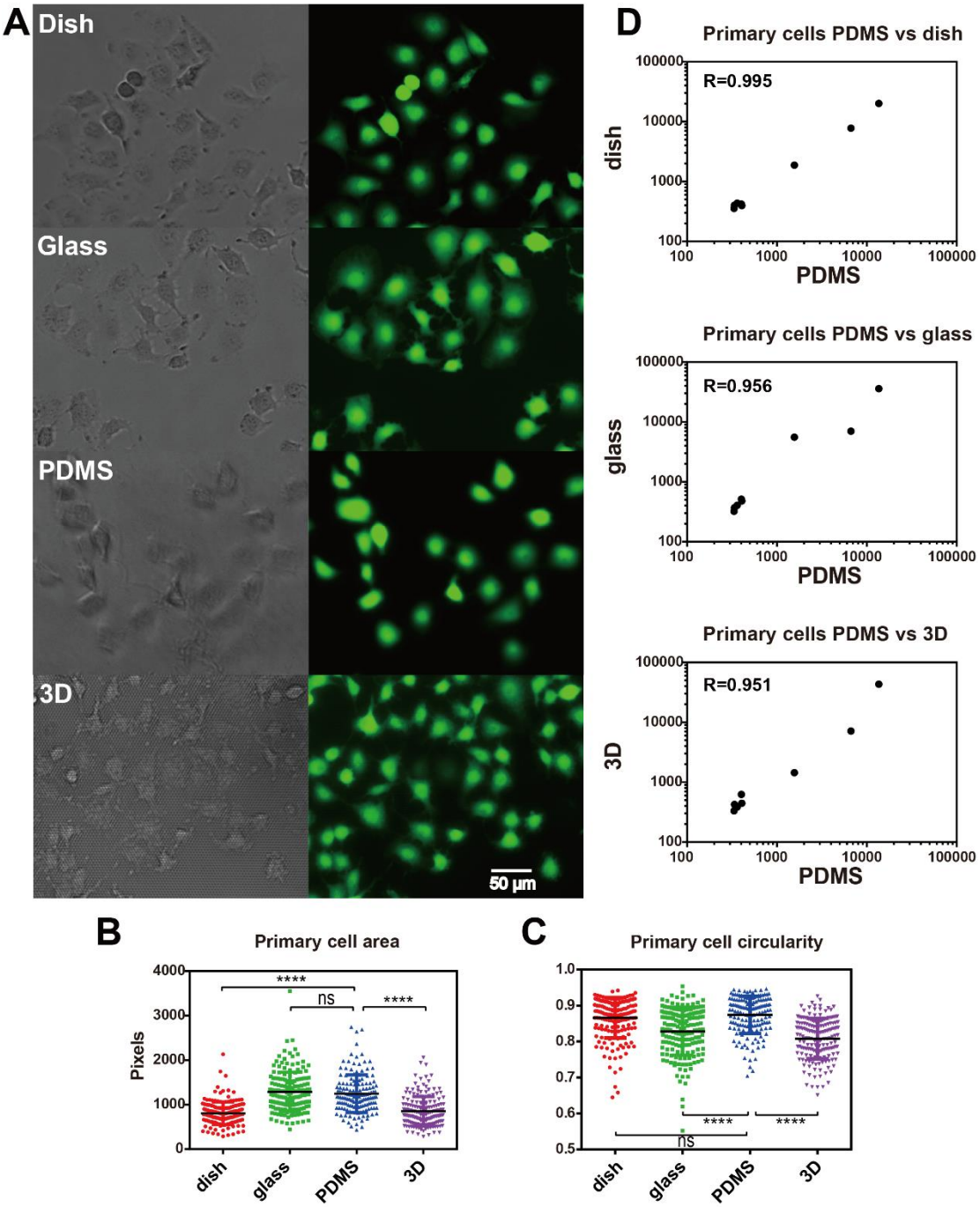


**Figure S8.** Comparison of OSCC primary cells cultured at different substrates, A-C, Morphology analysis of the cells, including A: optical & viability fluorescence staining; B: spread area, and C: cell circularity (n=172, 171, 151, 174 for Petri dish, glass, sealed PDMS chamber, and 3D culture plate (SCIVAX's NanoCulture Plate)). D, bulk level secretion analysis (including $^{CD63+}$EV, $^{CD9+CD63+}$EV, $^{CD81+CD63+}$EV, $^{EpCAM+CD63+}$EV, $^{HSP70+CD63+}$EV, IL-8, IL-6, and MCP-1), which showed there're no significant differences in secretion between the OSCC primary cells cultured in sealed PDMS

chambers and the cells cultured on Petri dish, glass or 3D cell culture plate (P= 0.8639, 0.805, and 0.848, paired t-test) and they showed high correlation with each other (R=0.995, 0.956, and 0.951).

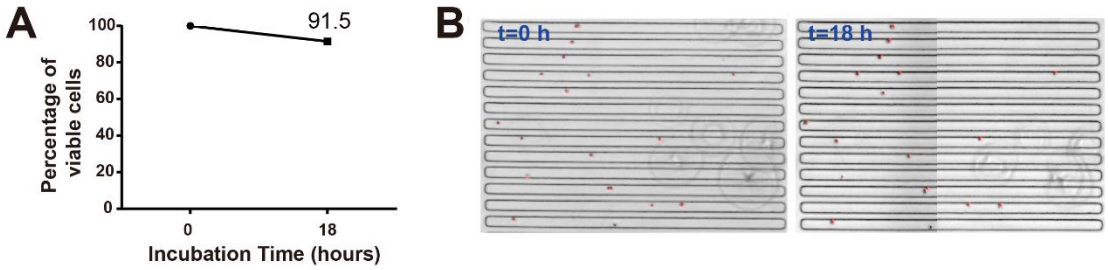


**Figure S9.** Cell viability analysis. The SCC25 cells were stained with cell tracker dye DiD (Thermo Fisher Scientific Inc., USA) before loading into PDMS microchambers to be incubated for 18 h. The cells showing positive fluorescence signal were scored as viable. A, Over 90% of the cells were still alive (n=445). B, Representative image comparing the same cells before and after incubation.

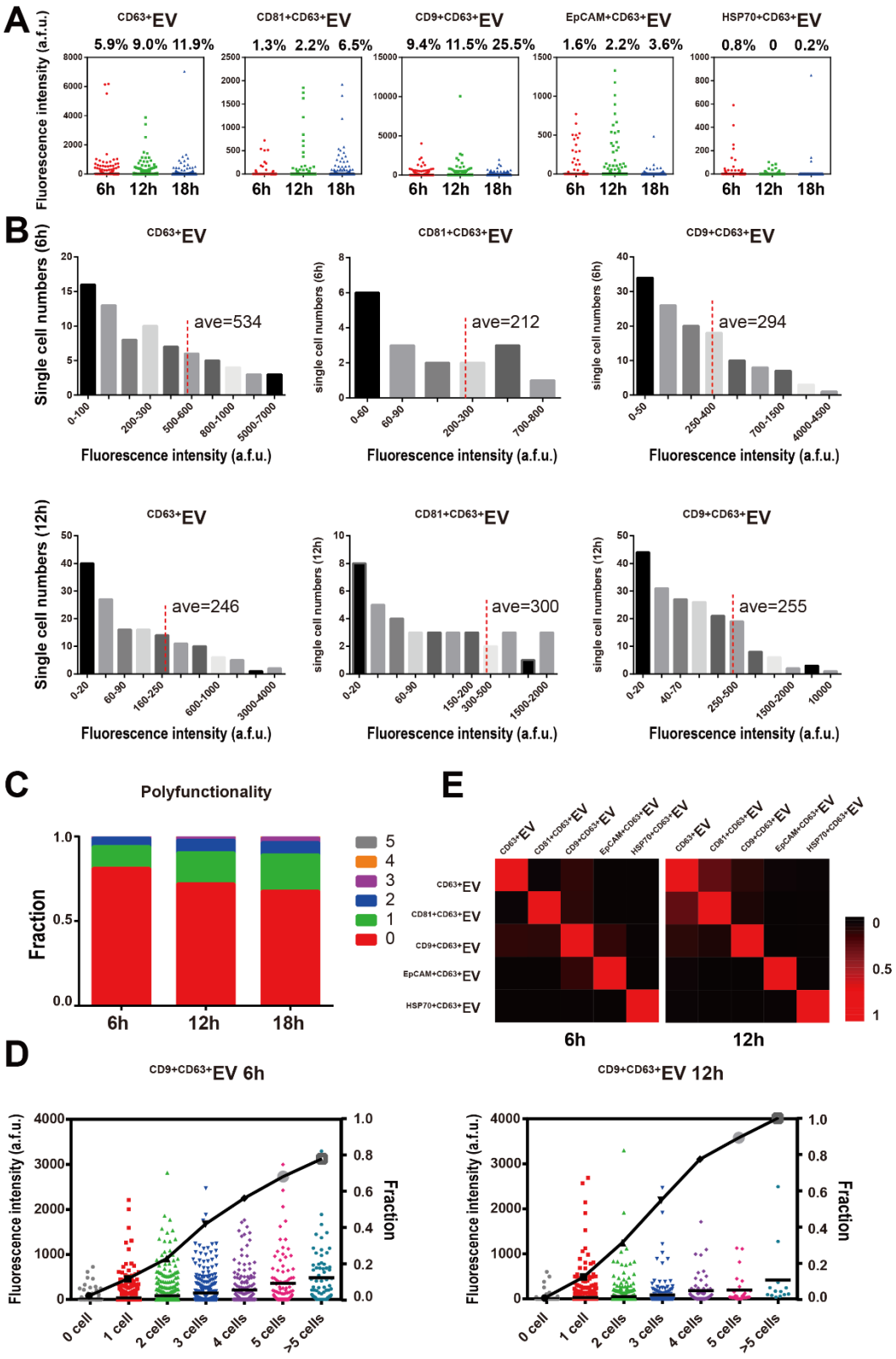


**Figure S10.** SCC25 single cell secretion analysis reveals intrinsic cell heterogeneity at different time points. A, Scatter plots comparing sing cell EV secretion frequencies at different time points (6 h, 12h, and 18 h). B, Histograms showing secretion intensity

distribution of different EVs ($C^{CD63+}$EV, $^{CD81+CD63+}$EV, and $^{CD9+CD63+}$EV) at 6 h and 12 h. The results show that a very small number of cells could secrete ~10 times more than average secretion, which confirms our observation from single cell EV secretion analysis at 18 h. C, Poly-functionality analysis reveals that cells became more poly-functional with the increased incubation time. D, Scatter plots showing the change of $^{CD9+CD63+}$EV secretion frequency with the increased number of cells per microchamber at 6 h and 12 h. E, Heatmaps showing the correlation between different EVs at single cell level at different profiling time window.

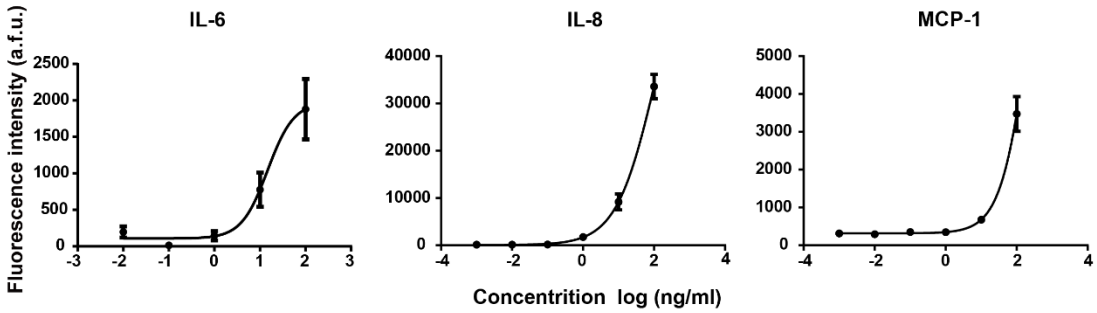


**Figure S11.** Calibration curves obtained with corresponding recombinant proteins (x, y-axes: log-scaled). These titration curves have been fitted with a 4PL curve and the fluorescence intensities presented were averaged from 8 spots for each protein.

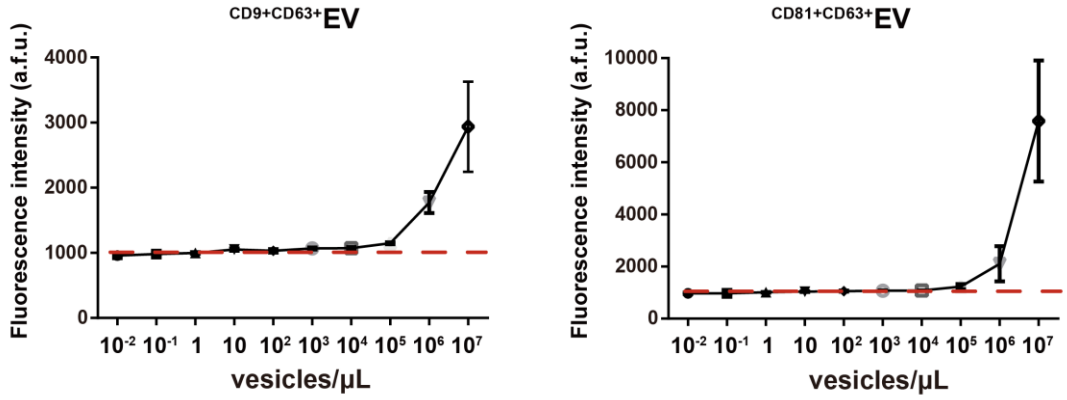


**Figure S12.** Titration curves for $^{CD9+CD63+}$EV and $^{CD81+CD63+}$EV. The titration curves were obtained using EV standard (ExoStd™ Lyophilized Exosome Standard, Biovision, USA) on antibody barcodes glass slides (the ones also used for single cell assay). The antibody barcodes glass side was bonded with PDMS microchannel array slab and

blocked with 1% BSA solution for 1 h. EV standards with different concentrations were added and incubated. After that, standard immunoassay procedures were performed to obtain detectable sandwich complex. The fluorescence results were read and analyzed with Genepix scanner and software. Fluorescence intensity represents the original photon counts averaged from 6 spots. From the titration curves, we can see the lowest detection concentration for $^{CD9+CD63+}$EV and $^{CD81+CD63+}$EV is ~$10^5$ EVs $\mu L^{-1}$. Considering the volume of each microchamber in single cell assay is ~1.7 nL, the lowest detectable number of EV is around 200 vesicles per microchamber.

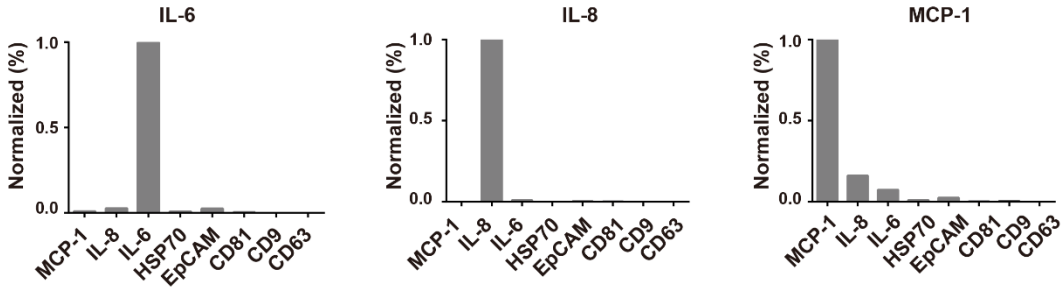


**Figure S13.** Cross-reactivity test. Most of the antibodies used in this study are monoclonal antibodies to ensure good specificity and reduce cross-reaction. The test was conducted by spiking a single recombinant protein solution (100 ng/mL) to antibody barcodes containing all capture antibodies, followed by detection with a mixture of detection Abs (IL-6, IL-8, MCP-1, and CD63). The fluorescence intensity was normalized into a percentage.

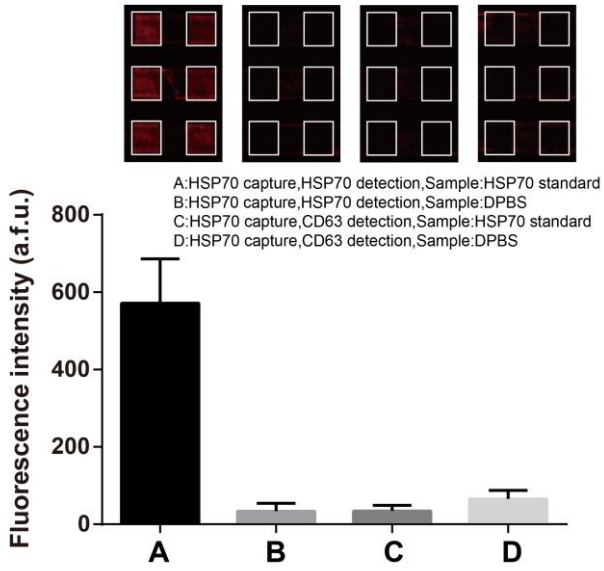


**Figure S14.** Validation of cross-reactivity test with HSP70 recombinant protein. The test was conducted by spiking HSP70 recombinant protein solution to HSP70 antibody barcode, followed by detection with different detection antibodies (biotinylated anti-HSP70 and biotinylated anti-CD63, respectively) and fluorescence staining.

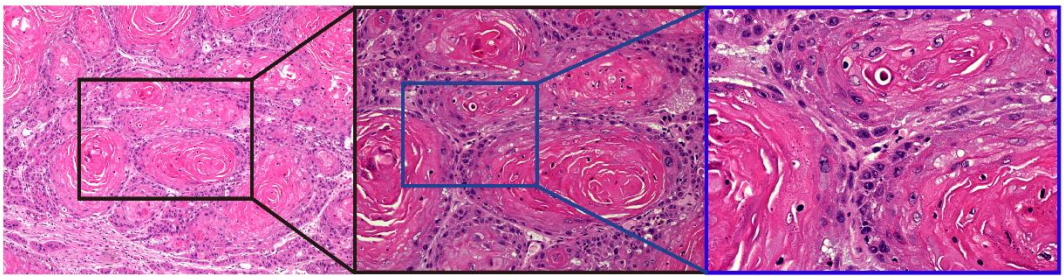

**Figure S15.** HE staining of patient 3 tissue showed highly differentiated oral squamous cell carcinoma. We observed the intercellular bridges, keratin pearl, and a few mitoses, while the nucleus and cell pleomorphic were not obvious.

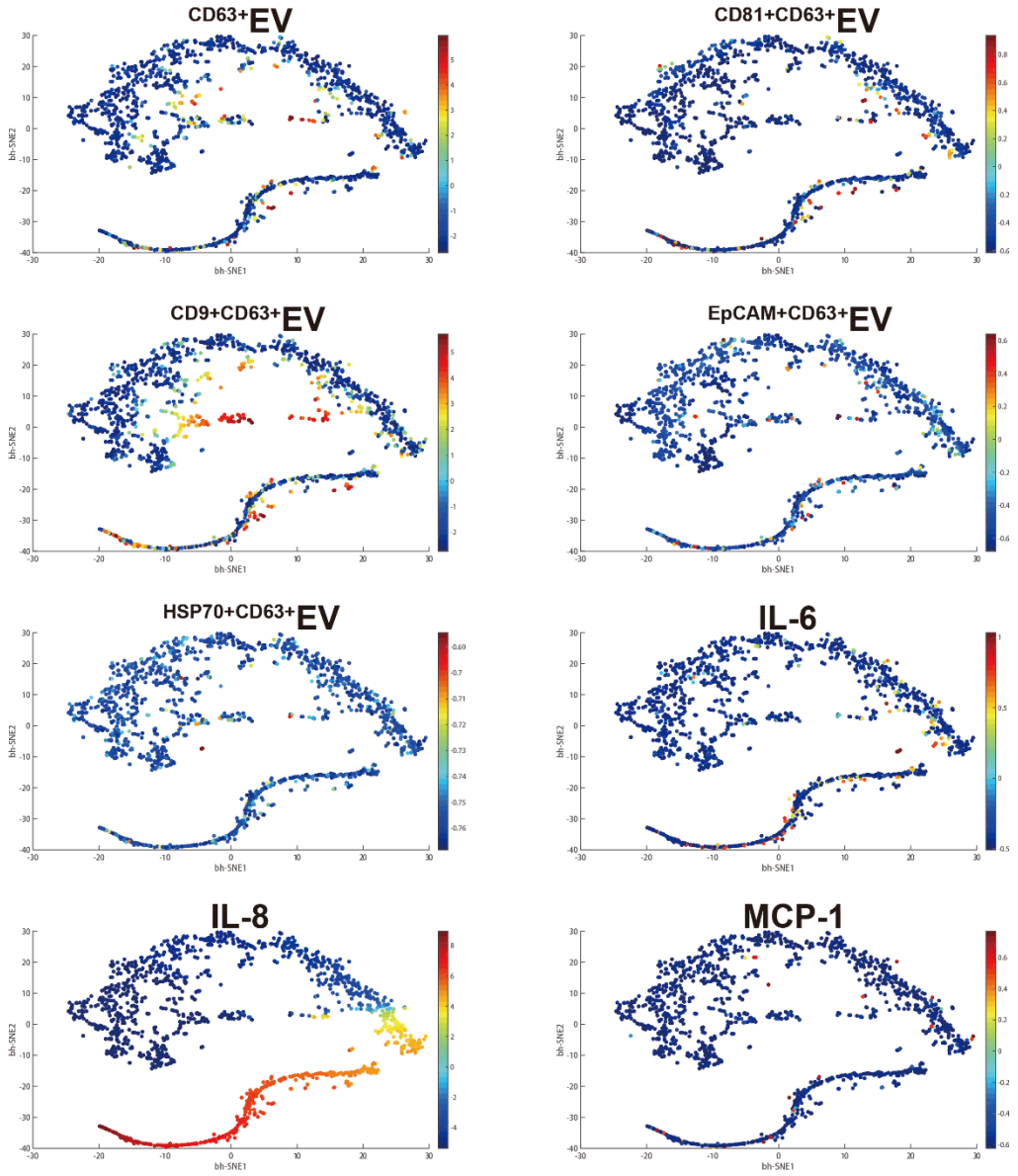


**Figure S16.** EV and protein distribution in the viSNE maps for SCC25 single cells.

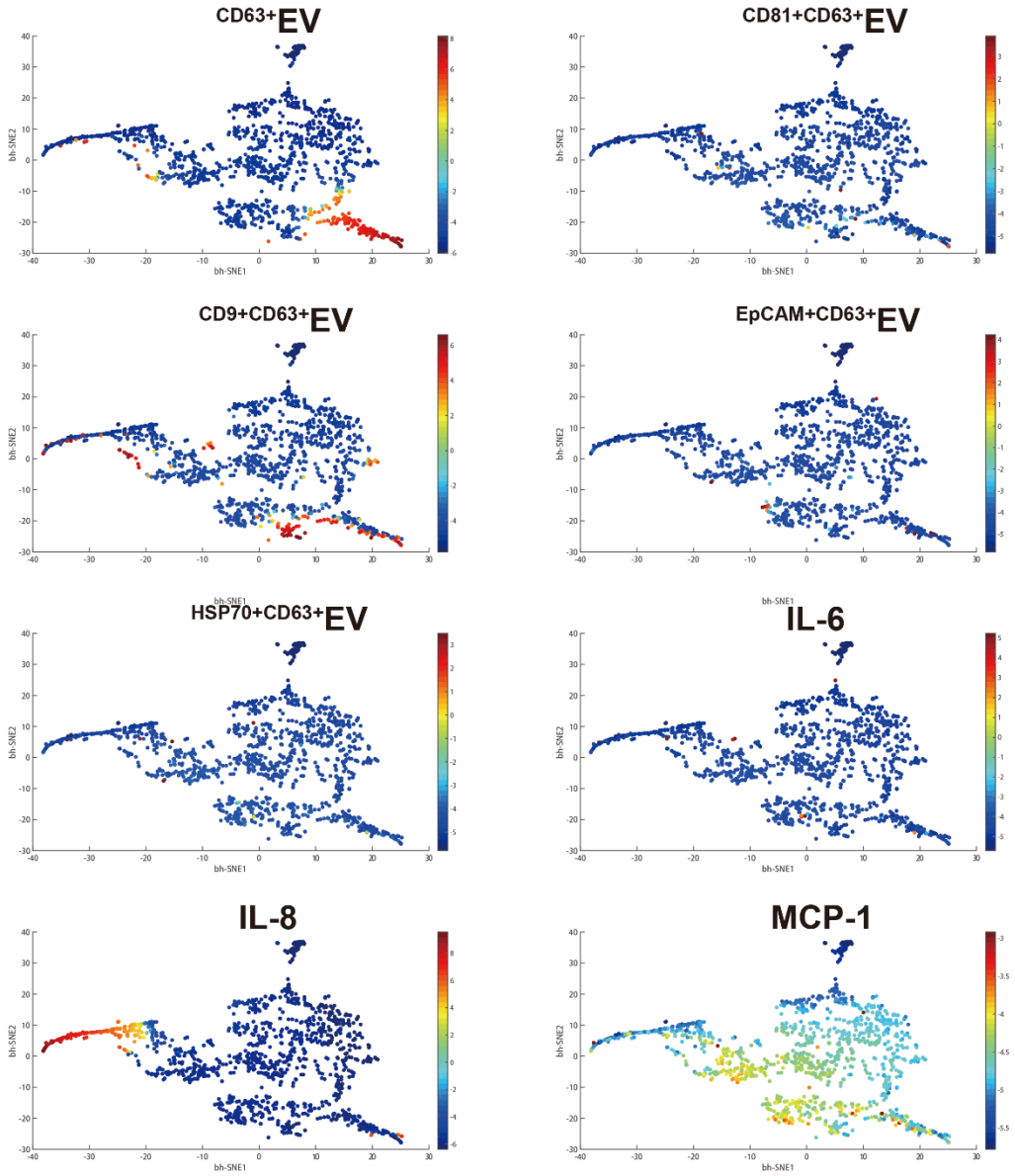


**Figure S17.** Whole panel secretion distribution in the viSNE maps for UM-SCC6 single cells.

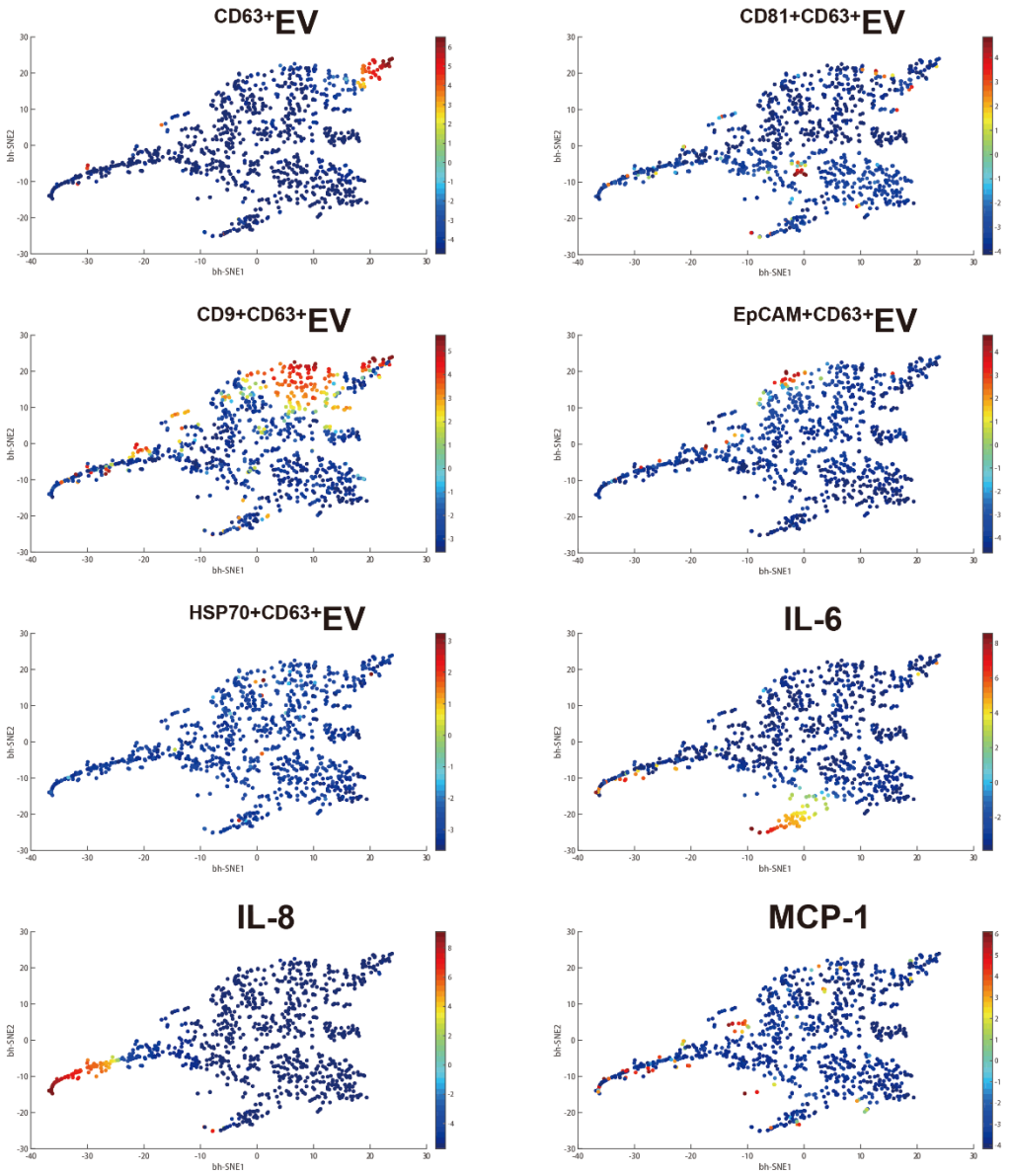


**Figure S18.** EV and proteins distribution in the viSNE maps for Patient 1.

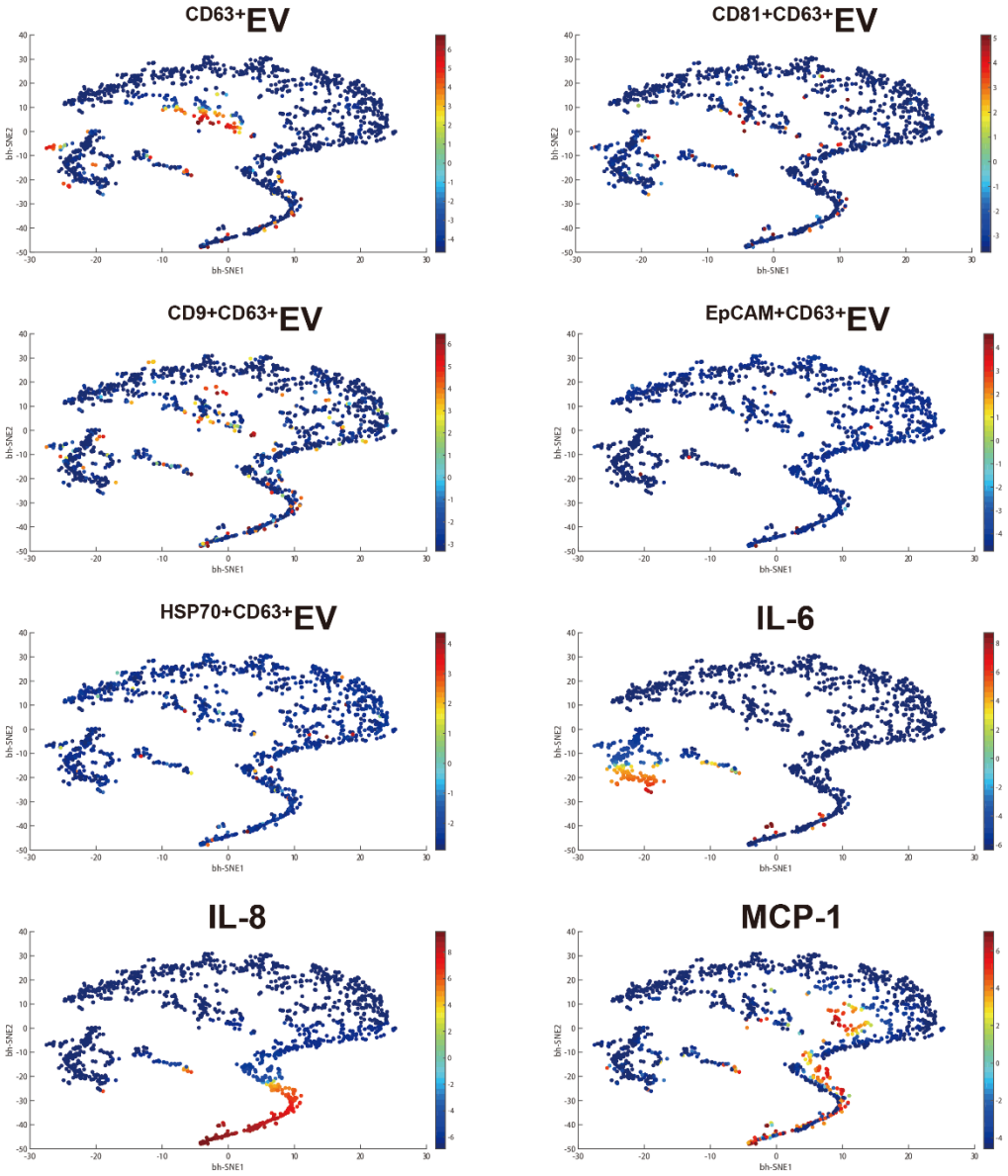


**Figure S19.** EV and proteins distribution in the viSNE maps for Patient 2.

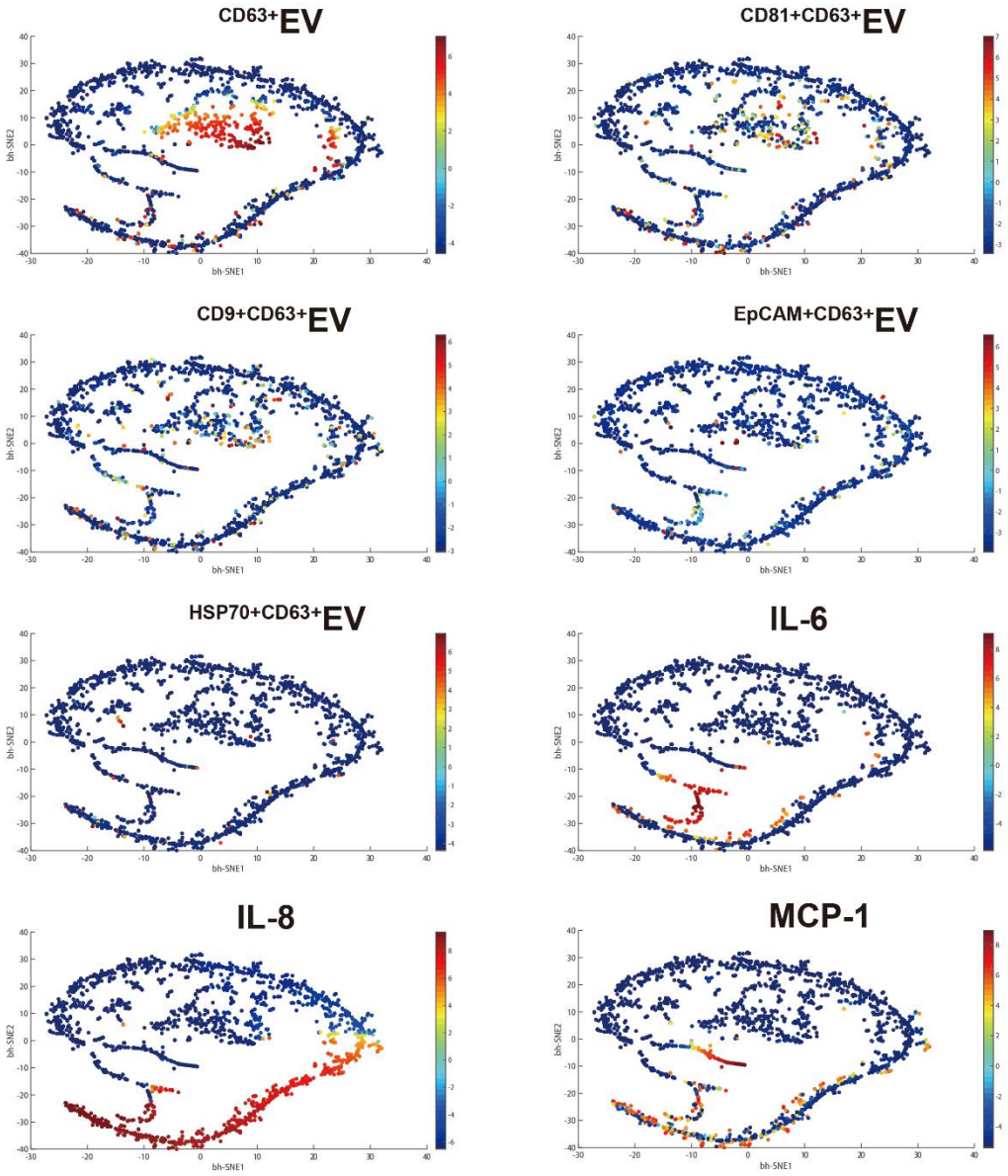


**Figure S20.** EV and proteins distribution in the viSNE maps for Patient 3.

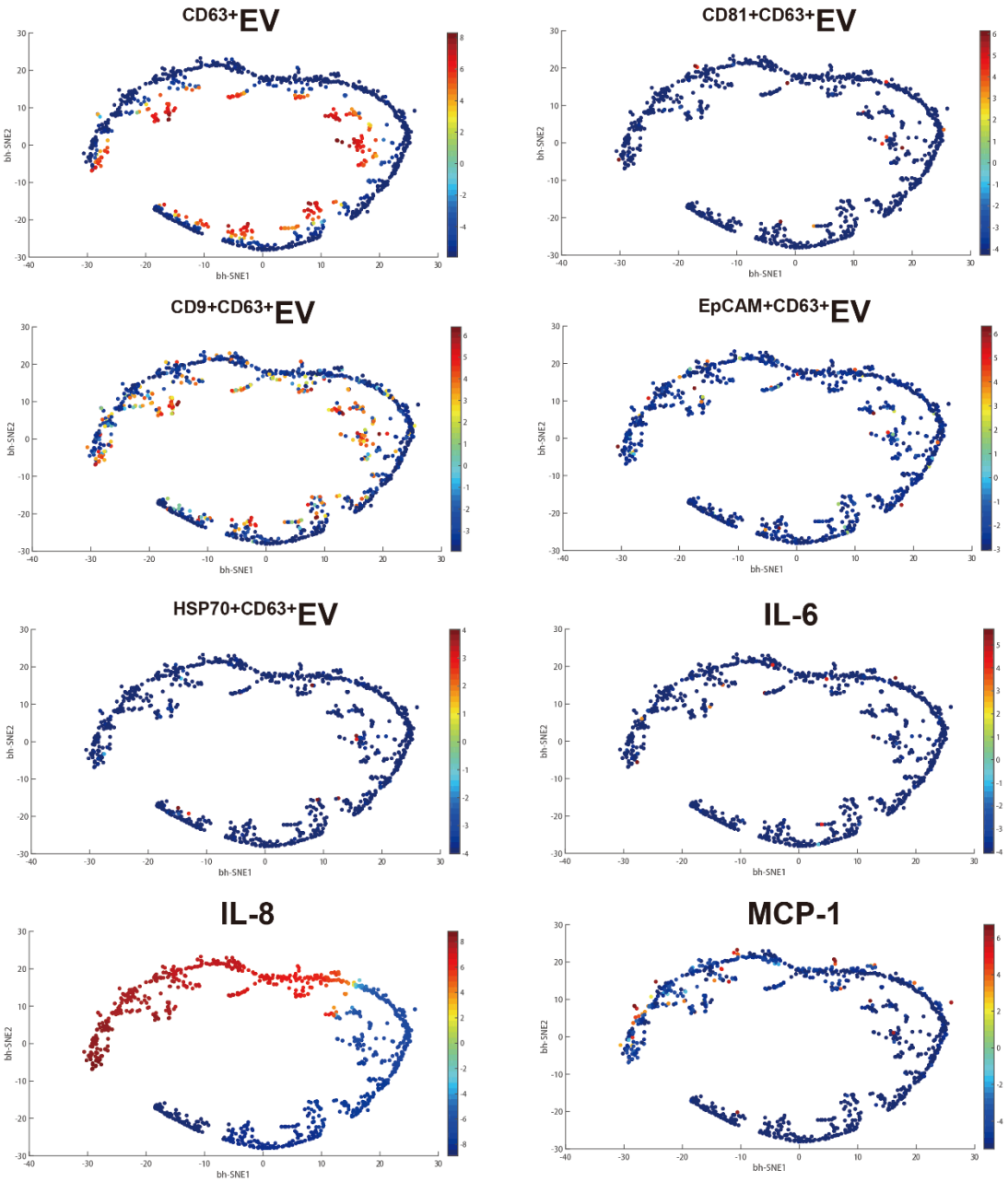


**Figure S21.** EV and proteins distribution in the viSNE maps for Patient 4.

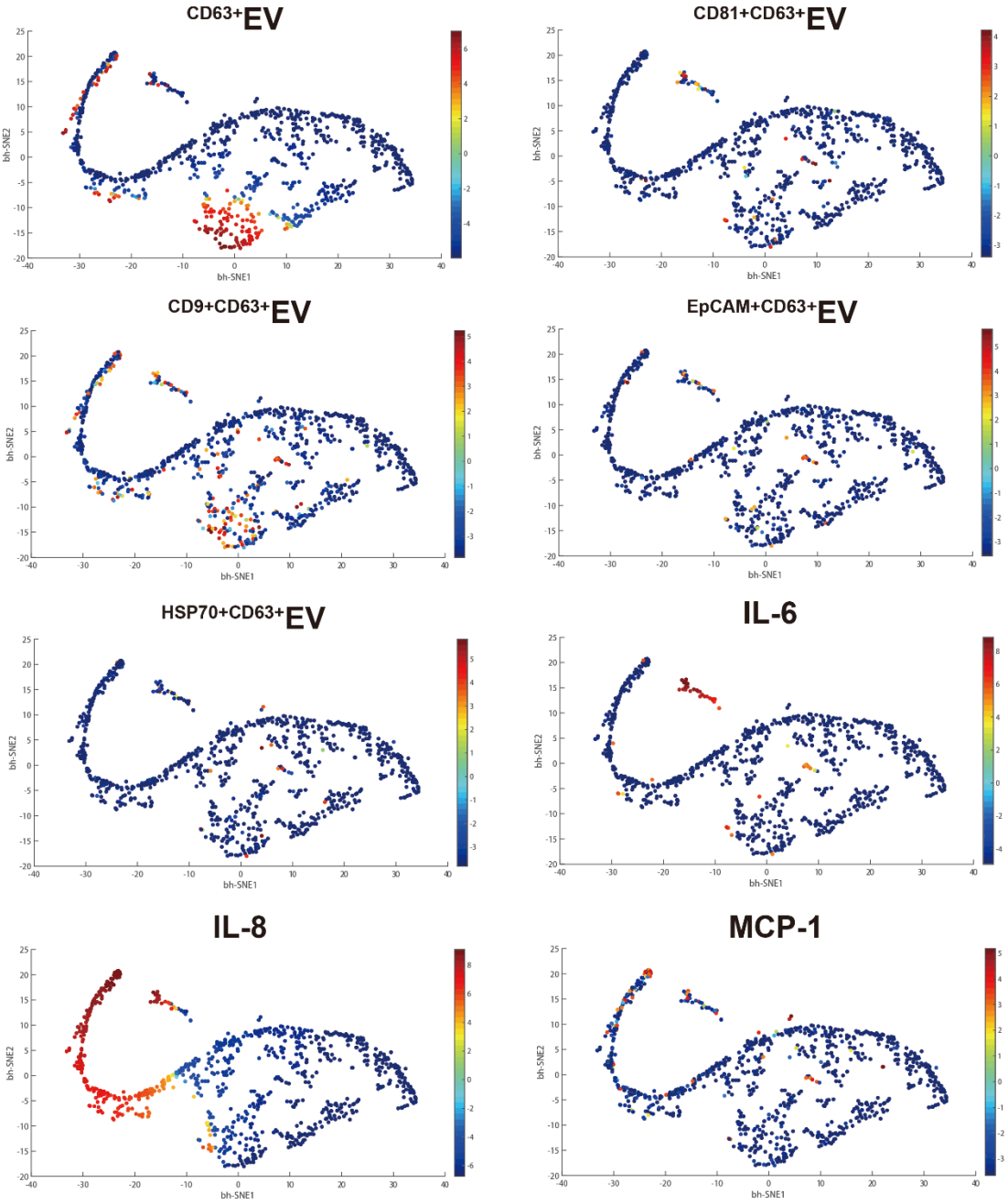


**Figure S22.** EV and proteins distribution in the viSNE maps for Patient 5.

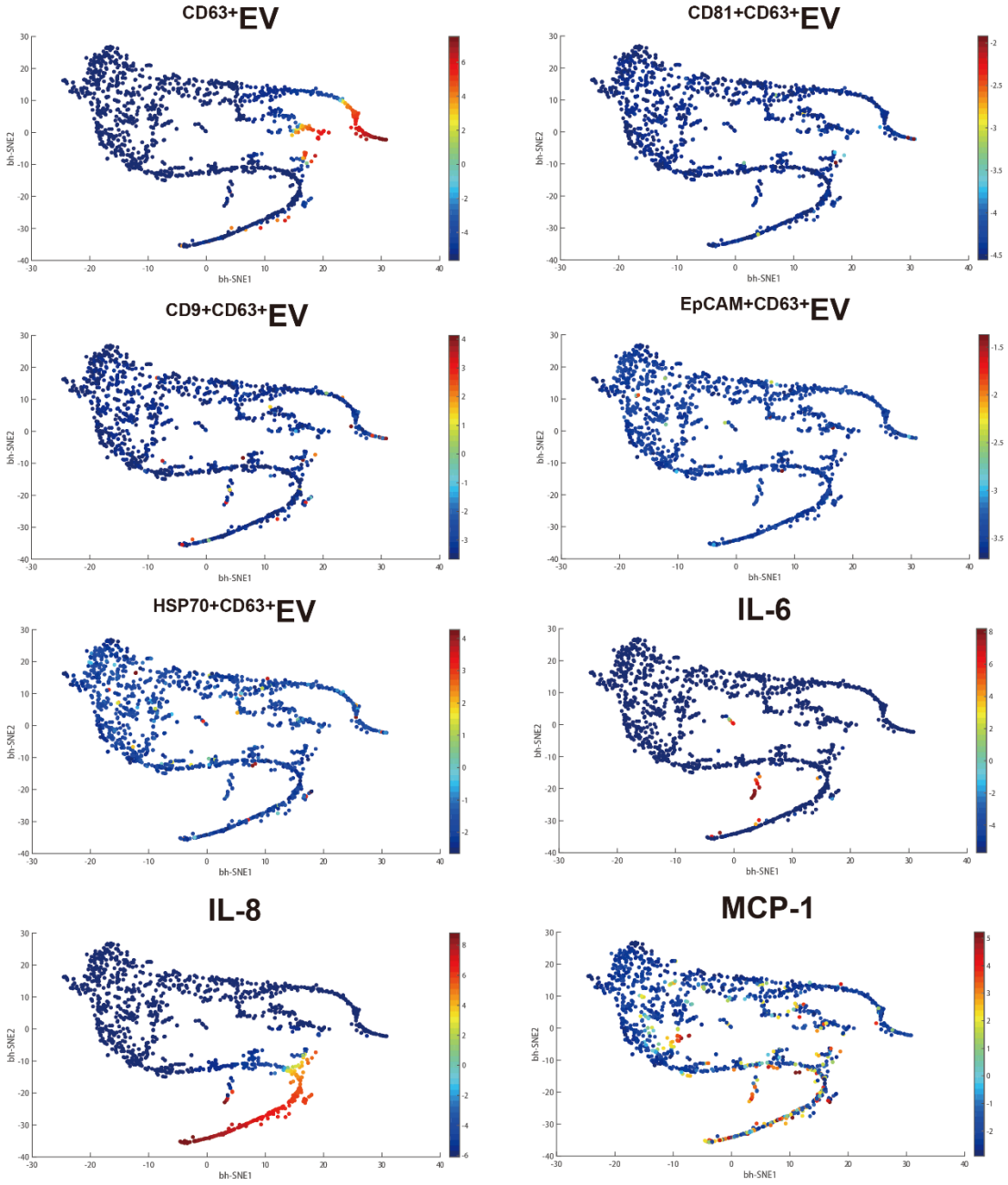


**Figure S23.** EV and proteins distribution in the viSNE maps for Patient 6.

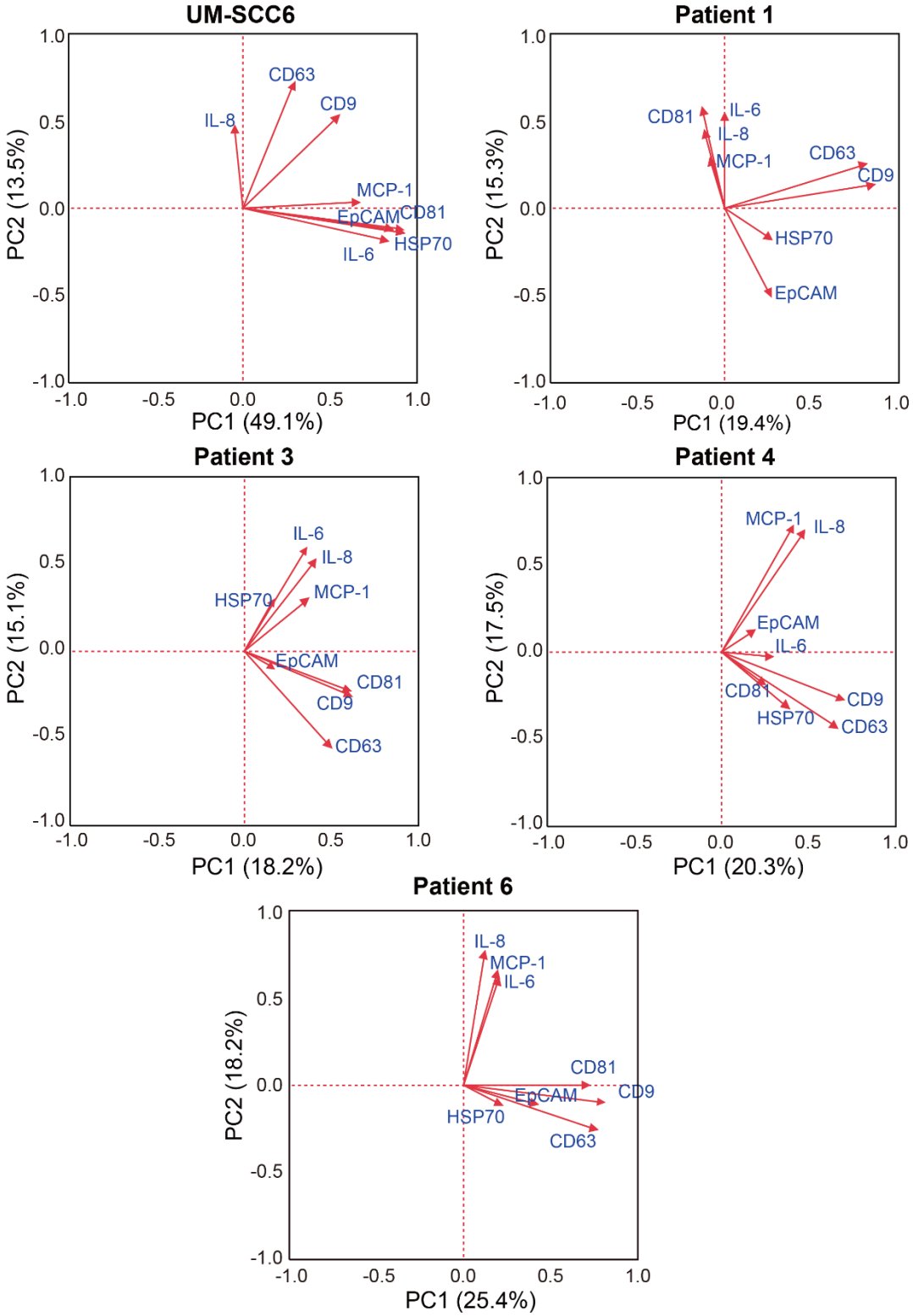


**Figure S24.** PCA analysis reveals that UM-SCC6, patient1&3&4&6 cells were also resolved into tiered clusters dictated differently by cytokines or EVs.

# Supplementary Tables

| Protein | company | Catalog number |
|---|---|---|
| Human CD9 | Millipore | CBL162 |
| CD63 | Millipore | CBL553 |
| CD81 | Novus Biologicals | NB100-65805 |
| EpCAM | Proteintech | 66316-I-Ig |
| HSP70 | R&D | DYC1663-5 |
| Human IL-6 | eBioscience | 88-7106-88 |
| Human IL-8 | eBioscience | 88-8086-88 |
| Human MCP-1 | eBioscience | 88-8337-88 |
| Biotin-CD63 | Biolegend | 353017-50 |
| Streptavidin-APC | eBioscience | 17-4317-82 |
| Streptavidin-PE | eBioscience | 12-4317-87 |

**Table S1.** Summary of antibodies used.

| Protein | Function |
|---|---|
| CD63 | Tetraspanins.<br>Inhibits metastasis.<br>Platelet activation. |
| CD81 | Tetraspanins.<br>Regulate cell activation and growth and cell aggregation.<br>Induce B cell adhesion and T cell development. |
| CD9 | Tetraspanins.<br>Metastasis suppressing.<br>Regulate Wnt signaling. Adhesion, platelet activation, B cell development. |
| EpCAM | Tumor-associated marker.<br>Induce genes involved in cellular metabolism, migration, proliferation, and differentiation. |
| HSP70 | Maintain cellular homeostasis; promote cell survival in response to stressful cellular conditions |
| IL-6 | Both a pro-inflammatory cytokine and an anti-inflammatory cytokine. Acute phase response.<br>play a role in host defense, acute phase reactions, immune responses, and hematopoiesis. |

| | |
|---|---|
| IL-8 | Chemotaxis<br>promote neutrophil chemotaxis and degranulation. |
| MCP-1 | Recruits monocytes, memory T cells, and dendritic cells.<br>Regulate adhesion molecule expression and cytokine production in monocytes. |

**Table S2.** List of all proteins used and their functions in human physiology.

| Patient | Gender | Age | Tumor type | Location | Differentiation | Metastasis |
|---|---|---|---|---|---|---|
| 1 | Male | 55 | OSCC | Mouth floor | high | Yes(cervical lymph node) |
| 2 | Male | 38 | OSCC | tongue | high | Yes(submandibular, deep cervical lymph) |
| 3 | Male | 60 | OSCC | tongue | high | No |
| 4 | Female | 65 | OSCC | tongue | high or medium | No |
| 5 | Male | 49 | OSCC | tongue | high | No |
| 6 | Male | 48 | OSCC | tongue | medium | Yes |

**Table S3.** A brief summary of the patients' medical records.